Eur. Phys. J. B **11**, 65–73 (1999)

THE EUROPEAN PHYSICAL JOURNAL B

EDP Sciences

Improvement of absolute band gaps in 2D photonic crystals by anisotropy in dielectricity

Zhi-Yuan Li[1,a], Ben-Yuan Gu[2], and Guo-Zhen Yang[2]

[1] Institute of Physics, Chinese Academy of Sciences, P. O. Box 603, Beijing 100080, P.R. China
[2] CCAST (World Laboratory), P.O. Box 8730, Beijing 100080, P.R. China

Received 26 January 1999

Abstract. Two–dimensional (2D) photonic band gaps (PBG) structure fabricated from anisotropic dielectric is studied by solving Maxwell's equations with use of plane–wave expansion method. Numerical simulations show that absolute photonic band gaps can be substantially improved in two dimensional square and triangular lattices of cylinders by introducing anisotropy in material dielectricity. Owing to different refractive indices for electromagnetic waves with E- and H-polarization, the quasi–independent adjustment of band gaps for the E- and H-polarization modes can be implemented by uniaxial crystals with their extraordinary axis parallel to the cylinders. Large absolute band gaps can be created for uniaxial cylinders in air with a positive anisotropy. In the case of air holes in background uniaxial dielectric with even a weak negative anisotropy, the absolute band gap can be increased 2-3 times. Large absolute band gap can also be obtained in other complex configurations of uniaxial and biaxial materials and this enables a full exploitation of potential utilization for anisotropic materials available in nature. Such a mechanism of band gap adjustment should open up a new scope for designing band gaps in 2D PBG structures.

PACS. 78.20.Ci Optical constants (refractive index, complex dielectric constant, absorption, reflection and transmission coefficients, emissivity) – 78.20.Fm Birefringence – 42.50.-p Quantum optics – 81.10.Aj Theory and models of crystal growth; physics of crystal growth, crystal morphology and orientation

1 Introduction

In the last decade there appears great interest in fabricating the photonic band gaps (PBG) structure (also called photonic crystals) [1–3] since the pioneering work of Yablonovitch and John [4,5]. These structures are periodic modulation of dielectric and will exhibit a "forbidden" frequency region where electromagnetic (EM) waves can not propagate for both polarizations along any directions. This may bring about some peculiar physical phenomena [4–9], as well as wide applications in several scientific and technical areas [1–3]. Although three–dimensional (3D) PBG structures will provide the most stirring potential in applications, the fabrication of such PBG structures with a band gap in the visible or infrared regime is exceedingly difficult and still remains a challenging task [10–14].

In contrast, it is much easier to fabricate two dimensional (2D) PBG structures in this regime [15–18]. Furthermore, 2D structures could also find some important uses such as a feedback mirror in laser diodes [19]. Perhaps for this reason, much attention has been drawn towards 2D PBG structures [20–26].

Since the superior features of PBG structures result from the photonic band gap, it is essential to design crystal structures with a band gap as large as possible. It is well known that the electromagnetic wave can be decomposed into the E- and H-polarization modes for a 2D structure. An absolute band gap exists for a 2D PBG crystal only when band gaps in both polarization modes are present and they overlap with each other. Thus it is our aim to search for some structures with an optimal overlapping band gap by varying parameters of the PBG structure, such as lattice type, refractive index contrast, filling fraction, and atom configurations.

It has recently been reported that the symmetry reduction of atom configuration by introducing two-point basis set in simple 2D lattices can remarkably increase absolute band gaps [27], quite similar to the 3D case with a nonspherical atom such as the diamond structure [11,28–31]. Recently, it was found that the anisotropy in atom dielectricity can also break the degeneracy of photonic bands such that partial band gaps can be created in face–centered cubic, body–centered cubic, and simple cubic lattices [32]. More recently, it was demonstrated that such an anisotropy in dielectricity can also remarkably increase absolute band gaps in 2D PBG structures [33].

The photonic band structure is left determined by the refractive index contrast, provided that other parameters

[a] e-mail: wangxh@aphy.iphy.ac.cn

as lattice type, filling fraction, and atom configuration are fixed. The sizes and positions of band gaps can be adjusted by varying the refractive index contrast. Thus, if we choose different refractive index contrasts for the E and H-polarization modes in a given PBG structure, we can match the relative position of band gaps for the two modes. This will enable the optimal overlapping of band gaps and the largest absolute band gap can be obtained. One way available is to fabricate PBG structures from materials with anisotropy in dielectricity. Nature offers a lot of anisotropic materials which are lossless and transparent in visible or infrared regime, among whom are uniaxial crystals and biaxial crystals.

In this paper, we will study the photonic band structures of 2D PBG structures fabricated from uniaxial and biaxial materials in their various configurations, and design the anisotropic PBG structure with an optimal absolute band gap. We first briefly introduce in Section 2 the plane–wave expansion method used in the calculations of photonic band structures for the E- and H-polarization modes of 2D anisotropic PBG structures. In Section 3, we investigate the general principle for improving the absolute band gap of PBG structures by anisotropic materials. Then in Section 4 we demonstrate the quasi–independent adjustment of band gaps for the E and H-polarization modes by uniaxial crystals with their extraordinary axis parallel to the cylinders. In Section 5 we will study the absolute band gap in other more complex configurations of anisotropic materials, in order to make a full exploitation of potential utilization for the available anisotropic materials in nature. Some brief summaries and conclusions are given in Section 6.

2 Model and formalism for anisotropic 2D photonic crystals

It is well–known in general optics that the uniaxial material has two different principal-refractive indices as ordinary-refractive index $n_{\rm o}$ and extraordinary-refractive index $n_{\rm e}$, while the biaxial crystal has three different principal refractive indices, namely, $n_x \neq n_y \neq n_z$. For such anisotropic materials, the dielectric constant ϵ is a dyadic (second rank tensor). In the principal coordinates where the Z-axis is parallel to the cylinders of 2D PBG structures, and the Bloch waves propagate in the XOY plane, the diagonal elements of ϵ are related to the principal-refractive indices as

$$\epsilon_{xx} = n_x^2, \quad \epsilon_{yy} = n_y^2, \quad \epsilon_{zz} = n_z^2,$$

while other dyadic elements are all zero.

To derive the eigen equations for 2D anisotropic PBG structures, we start from the case of 3D anisotropic PBG structures. In a periodic anisotropic structure where the dielectric constant $\epsilon(\mathbf{r})$ is a dyadic and position dependent, Maxwell's equations can reduce to the following equation satisfied by the magnetic field $\mathbf{H}$ as [32]

$$\nabla \times \left[\epsilon^{-1}(\mathbf{r}) \cdot (\nabla \times \mathbf{H})\right] = \frac{\omega^2}{c^2}\mathbf{H}, \tag{1}$$

where $\epsilon^{-1}(\mathbf{r})$ is the inverse dyadic of $\epsilon(\mathbf{r})$. Since $\epsilon(\mathbf{r})$ is periodic, we can use Bloch's theorem to expand both the $\mathbf{H}$ field and $\epsilon(\mathbf{r})$ in terms of plane waves, then from equation (1) we can obtain the following linear matrix equations for the dispersion of EM waves as

$$\sum_{\mathbf{G}',\lambda'} H^{\lambda,\lambda'}_{\mathbf{G},\mathbf{G}'} h_{\mathbf{G}',\lambda'} = \frac{\omega^2}{c^2} h_{\mathbf{G},\lambda}, \tag{2}$$

where

$$H^{\lambda,\lambda'}_{\mathbf{G},\mathbf{G}'} = \mid \mathbf{k}+\mathbf{G} \mid \quad \mid \mathbf{k}+\mathbf{G}' \mid \times \begin{pmatrix} \hat{\mathbf{e}}_2 \cdot \epsilon^{-1}_{\mathbf{G},\mathbf{G}'} \cdot \hat{\mathbf{e}}_{2'} & -\hat{\mathbf{e}}_2 \cdot \epsilon^{-1}_{\mathbf{G},\mathbf{G}'} \cdot \hat{\mathbf{e}}_{1'} \\ -\hat{\mathbf{e}}_1 \cdot \epsilon^{-1}_{\mathbf{G},\mathbf{G}'} \cdot \hat{\mathbf{e}}_{2'} & \hat{\mathbf{e}}_1 \cdot \epsilon^{-1}_{\mathbf{G},\mathbf{G}'} \cdot \hat{\mathbf{e}}_{1'} \end{pmatrix}. \tag{3}$$

Here the Fourier transform coefficient $\epsilon^{-1}_{\mathbf{G},\mathbf{G}'} = \epsilon^{-1}(\mathbf{G}-\mathbf{G}')$ is also a dyadic, and $\hat{\mathbf{e}}_1, \hat{\mathbf{e}}_2$ are orthogonal unit vectors which are both perpendicular to wave vector $\mathbf{k}+\mathbf{G}$ because of the transverse character of magnetic field $\mathbf{H}$ (*i.e.* $\nabla \cdot \mathbf{H} = 0$).

In the case of 2D PBG structures, the Bloch wave propagates in the XOY plane and thus we can choose $\hat{\mathbf{e}}_1 = \hat{z}$, $\hat{\mathbf{e}}_2 = e_{21}\hat{x} + e_{22}\hat{y}$, then $\hat{\mathbf{e}}_1 \cdot \hat{\mathbf{e}}_{2'} = \hat{\mathbf{e}}_2 \cdot \hat{\mathbf{e}}_{1'} = 0$.

For the E-polarization mode, $H_z = 0$, then we have $h_{\mathbf{G},1} = 0$. After simple algebraic derivation, equation (2) reduces to the following linear matrix equations,

$$\sum_{\mathbf{G}'} \mid \mathbf{k}+\mathbf{G} \mid\mid \mathbf{k}+\mathbf{G}' \mid \epsilon^{-1}_{zz}(\mathbf{G}-\mathbf{G}') h_{\mathbf{G}',2} = \frac{\omega^2}{c^2} h_{\mathbf{G},2}. \tag{4}$$

For the H-polarization mode, $H_x = H_y = 0$, and $h_{\mathbf{G},2} = 0$. Then equation (2) reduces to the following linear equations as

$$\sum_{\mathbf{G}'} \mid \mathbf{k}+\mathbf{G} \mid\mid \mathbf{k}+\mathbf{G}' \mid [\epsilon^{-1}_{xx}(\mathbf{G}-\mathbf{G}')\ e_{21}e_{2'1} + \epsilon^{-1}_{yy}(\mathbf{G}-\mathbf{G}')\ e_{22}e_{2'2}] h_{\mathbf{G}',1} = \frac{\omega^2}{c^2} h_{\mathbf{G},1}. \tag{5}$$

It is evident that for isotropic PBG structures with $\epsilon^{-1}_{xx}(\mathbf{G}-\mathbf{G}') = \epsilon^{-1}_{yy}(\mathbf{G}-\mathbf{G}') = \epsilon^{-1}_{zz}(\mathbf{G}-\mathbf{G}') = \epsilon^{-1}(\mathbf{G}-\mathbf{G}')$, equations (4, 5) will reduce to the familiar forms in references [21,24,25].

In the simplest configuration of anisotropic materials, the 2D PBG structure is fabricated from uniaxial crystals and the extraordinary axis is parallel to the extension direction of cylinders. Then, we have $\epsilon^{-1}_{xx}(\mathbf{G}-\mathbf{G}') = \epsilon^{-1}_{yy}(\mathbf{G}-\mathbf{G}')$. As $(\mathbf{k}+\mathbf{G}) \perp \hat{\mathbf{e}}_2$ and $(\mathbf{k}+\mathbf{G}') \perp \hat{\mathbf{e}}_{2'}$, equation (5) can be simplified into a more concise form as

$$\sum_{\mathbf{G}'} (\mathbf{k}+\mathbf{G}) \cdot (\mathbf{k}+\mathbf{G}') \epsilon^{-1}_{xx}(\mathbf{G}-\mathbf{G}') h_{\mathbf{G}',1} = \frac{\omega^2}{c^2} h_{\mathbf{G},1}. \tag{6}$$

In this configuration, the eigen equations for the E- and H-polarization modes are the same as those for the isotropic PBG structures, respectively, except that the dielectric constants for the two modes are now different.

They are $n_{\rm e}^2$ for the E-polarization mode and $n_{\rm o}^2$ for the H-polarization mode. The anisotropic photonic band structures embodied in equations (4, 6) are solved using standard matrix diagonization techniques, which is also the same as in the case of isotropic PBG structures [21,24,25,28,29]. In our calculations, the results were obtained using 289 plane waves. The convergence accuracy for the several lowest photonic bands is better than 1%.

For more complex configurations that 2D PBG structures are fabricated either from uniaxial crystals with one of the ordinary axes parallel to the cylinders, or from biaxial crystals, the photonic band structures embodied in equation (4) for the E-polarization mode are also solved in the same way as in the case of isotropic PBG structures. In contrast, $\epsilon_{xx}^{-1}(\mathbf{G}-\mathbf{G}')$ and $\epsilon_{yy}^{-1}(\mathbf{G}-\mathbf{G}')$ in equation (5) for the H-polarization mode are now different. Because of such an anisotropy of dielectric constant, equation (5) does not conserve in some symmetry transform operations of the lattice. The reduction of crystal symmetry results in the inequivalence of the photonic band structures along previously equivalent directions in the Brillouin zone. To demonstrate the existence of a band gap for the H-polarization mode, one has to calculate the photonic band structure along high symmetry lines in various regions of the Brillouin zone. Another equivalent way is to investigate the photonic band structure along the symmetry lines in a fixed region of the Brillouin zone, while permuting the dielectric dyadic elements ϵ_{xx} and ϵ_{yy} [32]. In this paper we would like to adopt the latter method to treat the anisotropic photonic band structures for the H-polarization mode. We also adopt 289 plane wave in our calculations, and the convergence accuracy for the several lowest photonic bands is better than 1%, too.

3 General principle for creating large absolute band gaps in anisotropic photonic crystals

In order to design anisotropic 2D PBG structures with large absolute band gaps, we first discuss the general principle for creating absolute band gaps by the anisotropy of material dielectricity.

We start from 2D PBG structures fabricated from isotropic material. We first examine 2D PBG structures consisting of dielectric cylinders in air. The cylinders are arranged in triangular lattice. The photonic properties of isotropic structures have been studied and shown to exhibit band gaps for each of the two polarization modes [21]. However, there is some discrepancy about whether an absolute band gap is present. Our simulations demonstrate that band gaps in the two polarization modes do not overlap with each other, resulting in the absence of the absolute band gap. This can be clearly seen from Figure 1, which displays the band structures of two polarization modes for a triangular lattice of isotropic dielectric cylinders in air. The cylinders have a refractive index of $n = 3.6$ and a filling fraction of $f = 0.4$. Two band gaps open for the E-polarization mode (plotted in solid lines), *i.e.* the 1-2 band gap and 3-4 band gap. For the H-polarization mode (plotted in dotted lines) a band gap is opened between 1-2 bands. However, the H 1-2 band gap lies between the E 1-2 and 3-4 band gaps, thus no absolute band gap is present. Simulations at other filling fractions also show that no absolute band gap is opened as the higher edge of the H 1-2 band gap always coincides with the lower edge of the E 3-4 band gap at high refractive index. This can be attributed to the degeneracy between the H 2 band and E 3, 4 bands, as shown in Figure 1.

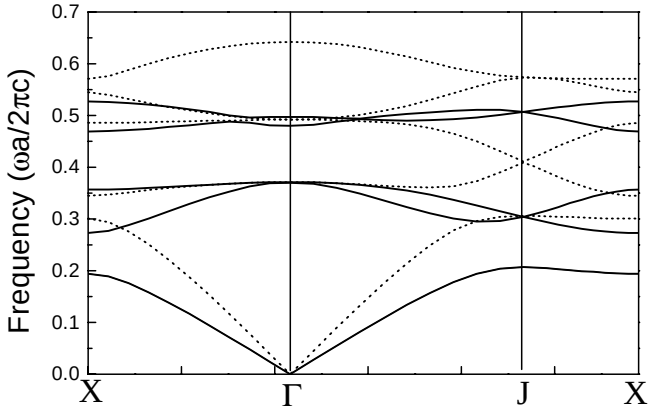

Fig. 1. Calculated photonic band structure for a triangular lattice of isotropic dielectric cylinders in air for E-polarization (solid lines) and H-polarization (dotted lines) modes. The cylinders have a refractive index of $n = 3.6$ and a filling fraction of $f = 0.4$.

The case can be changed by introducing the anisotropy in the dielectric of cylinders. For simplicity and not without generality, we prefer to choose uniaxial materials with their extraordinary axis parallel to the extension direction of cylinders. According to Figure 1, if we can move upwards the H 1-2 band gap so that it can overlap with the E 3-4 band gap, or if we can shift it downwards as to overlap with the E 1-2 band gap, an absolute band gap will be opened. As the photonic band frequency is somewhat inverse with respect to refractive index contrast, this means that we must choose in the former case a refractive index for the H-polarization mode lower than that for the E-polarization mode, namely, $n_{\rm e} > n_{\rm o}$, a positive uniaxial crystal. In the latter case, we should select a negative uniaxial material with $n_{\rm e} < n_{\rm o}$.

Following this idea, we investigate the dependence of band gap positions on the refractive index for both polarization modes, in order to design PBG structures with optimal band gaps. As an example, we first consider the triangular lattice of dielectric cylinders in air. The filling fraction of cylinders is fixed as $f = 0.4$. The results are displayed in Figure 2. A band gap is present for the H-polarization mode at a refractive index larger than 3.0. Two wide band gaps still open for the E-polarization mode at a refractive index as low as $n = 2.0$. However, the band gaps of the two modes do not overlap at all refractive indices. The top edge of the H 1-2 band gap is always lower than the bottom edge of the E 3-4 band gap, while the bottom edge of the H 1-2 band gap is always higher than

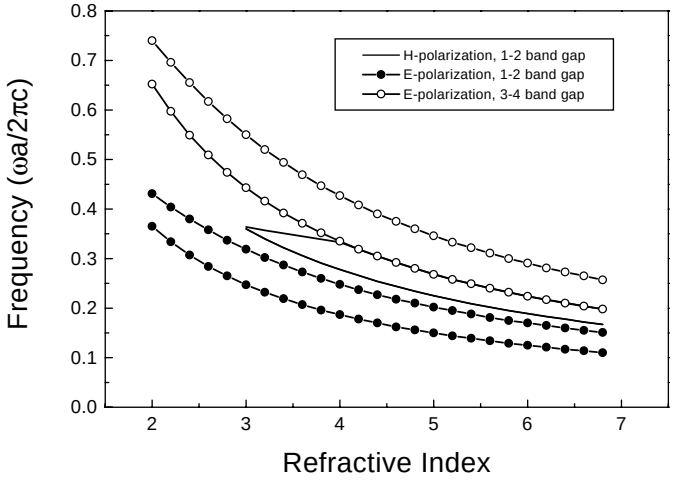

Fig. 2. Dependence of band gap positions on the refractive index for the triangular lattice of dielectric cylinders in air with a filling fraction of $f = 0.4$.

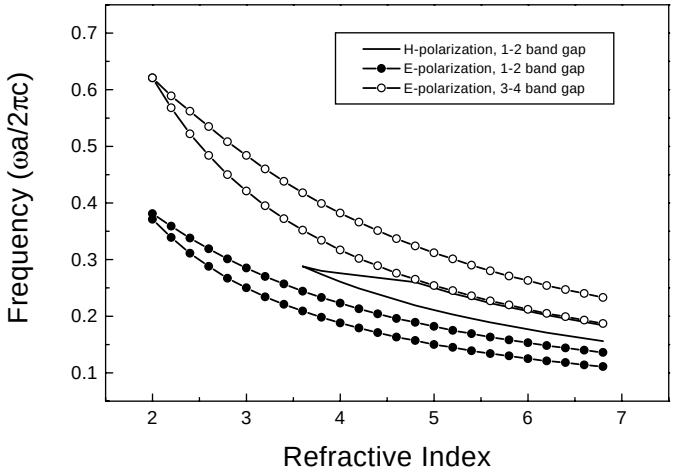

Fig. 3. Dependence of band gap positions on the refractive index for the square lattice of dielectric cylinders in air with a filling fraction of $f = 0.4$.

the top edge of the E 1-2 band gap. Therefore, no absolute band gap is present at all refractive indices.

As conceptualized above, the optimal overlap of E and H band gaps can be obtained by introducing anisotropy in material dielectricity. This is verified when one looks into Figure 2. The H 1-2 band gap can overlap either with the E 1-2 band gap at a lower refractive index or with the E 3-4 band gap at a higher refractive index. Given an anisotropy sufficient enough, the band gaps will match completely and the largest absolute band gap can be achieved. In particular, consider the large H 1-2 band gap at $n_o = 4.0$, which lies between $0.278 - 0.333$ $(2\pi c/a)$, c is the light speed in vacuum and a is the lattice constant of a triangular lattice. Its top edge overlaps with that of the E 3-4 band gap at $n_e = 5.2$, and its bottom edge overlaps with that of the E 3-4 band gap at $n_e = 4.8$. Therefore, the two band gaps overlap wholly each other at the range of $4.8 \leq n_e \leq 5.2$. Similarly, it can be found that this H 1-2 band gap also completely overlaps with the E 1-2 band gap at the range of $2.6 \leq n_e \leq 2.8$. The anisotropy to obtain the optimal absolute band gap by a positive crystal is weaker than that by a negative crystal, thus it is easier in experiment to fabricate from positive uniaxial material 2D PBG structures with optimal band gaps.

Such a concept is also applicable to other lattice types and atom configurations. Figure 3 displays the dependence of band gap positions on the refractive index contrast for both polarization modes in a square lattice of dielectric cylinders in air. The filling fraction of cylinders is fixed as $f = 0.4$. Although the band gap variations are similar to those in triangular lattice, comparing Figure 3 with Figure 2, the band gaps are narrower than in triangular lattice. The H 1-2 band gap does not open until at a large refractive index over 3.6, and reaches its maximum size at $n = 4.8$.

According to Figure 3, no absolute band gap is present in such isotropic PBG structures at any refractive index. However, an absolute band gap can also be opened by the introduction of sufficient anisotropy into material dielectricity, shifting the H 1-2 band gap either upwards or downwards to overlap with the E 3-4 band gap or the E 1-2 band gap, respectively. Similar to a triangular lattice, an optimal absolute band gap can be obtained by matching the relative position of the H 1-2 band gap either with the E 3-4 band gap or with the E 1-2 band gap, corresponding to the selection of positive crystals or negative crystals. Because of narrower E 1-2 and 3-4 band gaps, the matching condition is more strict than for triangular lattice. For example, the large H 1-2 band gap at $n_o = 4.8$ can completely overlap the E 3-4 band gap at the narrow range of $5.9 \leq n_e \leq 6.0$, and overlap the E 1-2 band gap only at about $n_e = 3.1$. It is also favorable to obtain from positive crystals the optimal absolute band gaps in such square lattice structures.

In principle the optimal absolute band gaps can be obtained for any 2D photonic crystals, as the quasi–independent adjustment of band structures by the anisotropy in dielectricity is so effective. However in practice, due to limited anisotropic materials [34], such an optimal match in band gaps can not fully be achieved because it needs very strong anisotropy in material dielectricity. Nevertheless, the anisotropy is still of much help to create and increase absolute band gaps in 2D PBG structures.

As to PBG structures with air cylinders in background dielectric, which exhibit absolute band gaps in both square and triangular lattices [3], the anisotropy in dielectricity can also improve the size of absolute band gap. The principle is essentially the same as in crystals of dielectric cylinders in air.

Figure 4 displays the dependence of band gap positions on the refractive index contrast for both polarization modes in a square lattice of air cylinders embedded in dielectric medium. The filling fraction of air holes is $f = 0.7$. It is evident that the H 2-3 band gap overlaps partially with the E 3-4 band gap at a refractive index of background medium larger than 2.8. Photonic crystals composed of negative material with a weak anisotropy will

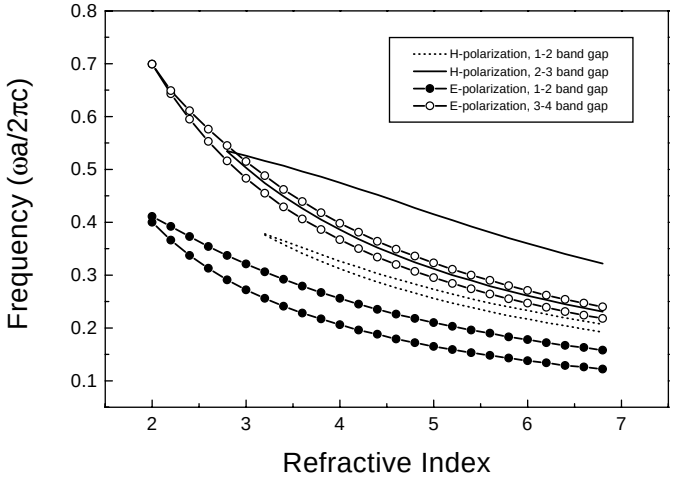

Fig. 4. Dependence of band gap positions on the refractive index for a square lattice of air cylinders in dielectric medium. The cylinders have a filling fraction of $f = 0.7$.

move upwards the E 3-4 band gap relative to the H 2-3 band gap. This will improve remarkably the two band gaps overlapping and the absolute band gap can be increased 2-3 times. As an example, the absolute band gap for isotropic PBG structure at $n = 4.0$ has a width of $\Delta\omega = 0.012(2\pi c/a)$. Yet the anisotropic PBG structure with $n_{\rm e} = 4.0$ and $n_{\rm o} \geq 4.2$ exhibits an absolute band gap with $\Delta\omega = 0.031(2\pi c/a)$, about three times the size of that in isotropic crystals. The E 3-4 and H 2-3 band gaps can be matched optimally by weak negative anisotropy in a wide range of refractive index. Yet it is difficult in practice to match the E 1-2 band gap with the H 2-3 band gap, as this will require very strong anisotropy in negative materials. Simulations made for the triangular lattice of air cylinders in background dielectric demonstrate that large absolute band gaps also open for anisotropic 2D PBG structures.

In the above we have shown that the anisotropy in material dielectricity for both square and triangular lattices can increase the size of absolute photonic band gap remarkably. As the refractive index for the E-polarization and H-polarization modes can be chosen different, the band gaps can be adjusted quasi–independently and matched to overlap optimally. In particular, the positive uniaxial materials are more favorable in improving the absolute band gap of PBG structures consisting of dielectric cylinders in air, while for crystals composed of air holes in dielectric medium, negative uniaxial materials are more competent. These general principles should be followed in the practical design of anisotropic 2D PBG structures with large absolute band gaps. Furthermore, they should be applicable to uniaxial and biaxial materials in various configurations of dielectricity.

4 Large absolute band gaps in uniaxial photonic crystals

According to the analyses in Section 3, materials with large refractive index and sufficient anisotropy are required in the creation of absolute band gaps in 2D anisotropic PBG structures. This may impose a severe restrictions on the anisotropic materials available in nature that can be effective candidates for PBG structures. As a practical example, we consider 2D PBG structures made from Te (tellurium), which is a kind of positive uniaxial crystal with unusually large principal indices of $n_{\rm e} = 6.2$ and $n_{\rm o} = 4.8$ in the wavelength regime between 3.5 μm and 35 μm. Although Te is a semiconductor material, the free carrier absorption is quite weak in the infrared regime with an absorption coefficient of $\alpha \simeq 1$ cm^{-1}. Thus, the imaginary parts of the complex refractive indices can be neglected compared with their real parts, and the photonic band structures will not be changed. Furthermore, the absorption will not become a serious problem as a PBG structure consisting of several tens of unit cell layers is thick enough for practical applications.

As noted in Section 3, the quasi–independent match of band gaps through anisotropy in the refractive index for the E- and H-polarization modes can be implemented most effectively and conveniently when the extraordinary axis of Te is chosen parallel to the extension direction of cylinders. Furthermore, as a positive crystal, Te is more favorable in improving the absolute band gap of PBG structures consisting of dielectric cylinders in air. This is verified by numerical simulations on photonic band structures. The photonic band structures for triangular and square lattices of Te cylinders in air are displayed in Figures 5a and 5b, respectively. In both lattices the filling fractions of cylinders are $f = 0.4$ and the extraordinary axis of Te is chosen parallel to the cylinders. It is evident that an absolute band gap is present in both lattice structures, which results from the overlap of the H 1-2 band gap with the E 3-4 band gap, consistent with the analysis of anisotropy match for band gaps shown in Figures 2 and 3. The absolute band gap (crosshatched region in Figs. 5a and 5b) for the triangular lattice has a width of $\Delta\omega = 0.046(2\pi c/a)$, and a band gap to midgap ratio of $\Delta\omega/\omega_{\rm g} = 17.9\%$. For the square lattice we have $\Delta\omega = 0.035(2\pi c/a)$ and $\Delta\omega/\omega_{\rm g} = 14.8\%$.

We next investigate the dependence of band gap positions on the filling fraction of Te cylinders for the E- and H-polarization modes. The results are displayed in Figures 6a and 6b for triangular and square lattices of Te cylinders in air, respectively. In both lattice structures, an absolute band gap resulting from the overlap of the H 1-2 band gap with the E 3-4 band gap persists in a wide range of filling fraction of Te cylinders. At a filling fraction of about $f \leq 0.36$, the H 1-2 band gap lies in the wide E 3-4 band gap, and at a larger filling fraction, the two band gaps intersect. Because of this variation character, the maximum absolute band gap lies at $f = 0.41$ for the triangular lattice with a band gap width of $\Delta\omega = 0.046(2\pi c/a)$ and a band gap to midgap ratio of $\Delta\omega/\omega_{\rm g} = 18.0\%$, and for the square lattice it lies at $f = 0.38$ with $\Delta\omega = 0.037(2\pi c/a)$ and $\Delta\omega/\omega_{\rm g} = 15.2\%$.

As to the 2D PBG structures composed of air holes in dielectric medium, negative uniaxial materials are more competent in improving the absolute band gap,

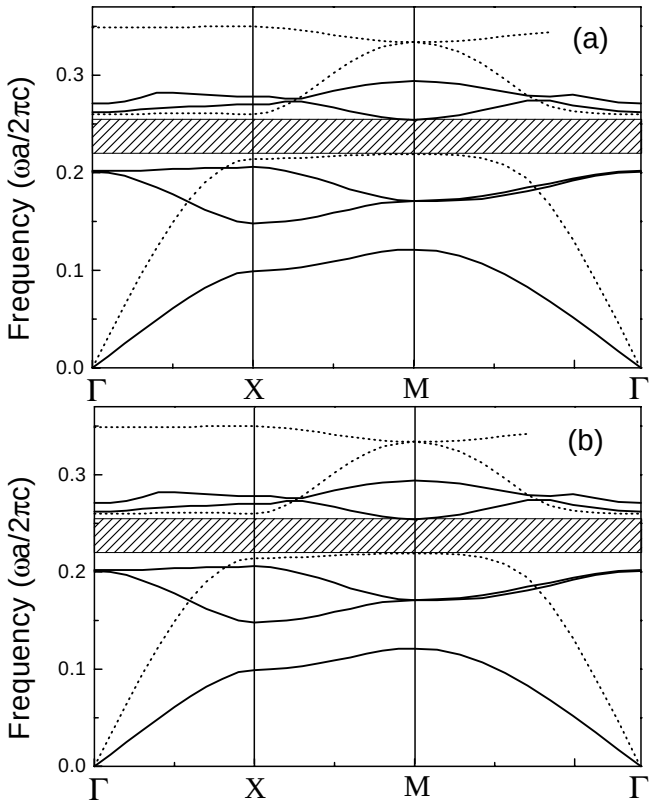

Fig. 5. Calculated photonic band structures of (a) a triangular lattice; and (b) a square lattice of Te cylinders in air for E-polarization (solid lines) and H-polarization (dotted lines) modes. The filling fractions of Te cylinders in both lattices are $f = 0.4$ and the extraordinary axis of Te is parallel to the cylinders. An absolute band gap (crosshatched region) is present between $0.234 - 0.280(2\pi c/a)$ in the triangular lattice and lies between $0.219 - 0.254(2\pi c/a)$ in the square lattice.

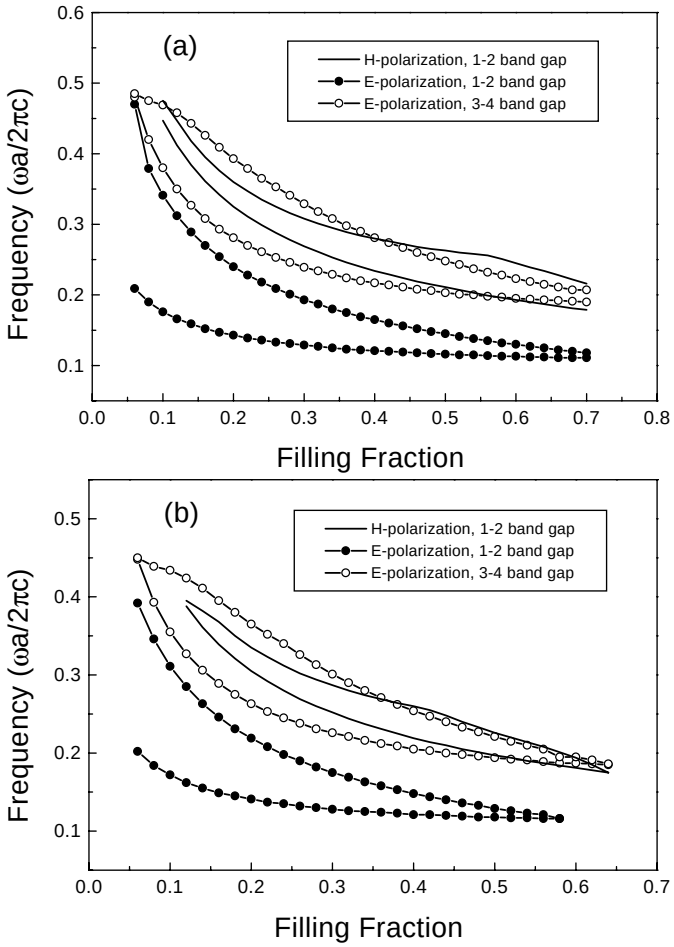

Fig. 6. Dependence of band gap positions on the filling fraction of Te cylinders for (a) a triangular lattice; and (b) a square lattice of Te cylinders in air. The extraordinary axis of Te is parallel to the cylinders.

according to the analyses made in Section 3. The material we consider is Tl_3AsSe_3, which is a negative uniaxial crystal with $n_o = 3.35$ and $n_e = 3.16$ in the visible regime. The anisotropy in dielectricity is not remarkable, however, according to Figure 3, it is sufficient to improve the size of absolute band gap in a square lattice of air holes by 2-3 times. We calculate the photonic band structures for square and triangular lattices of air cylinders in Tl_3AsSe_3 background medium, and the results are displayed in Figures 7a and 7b, respectively. The filling fractions of air cylinders are both $f = 0.7$ and the extraordinary axis of Tl_3AsSe_3 is also parallel to the cylinders axis. In the square lattice, the absolute band gap results from the overlap of the E 3-4 and H 2-3 band gaps, while in the triangular lattice it results from the overlap of the E 2-3 and H 1-2 band gaps. In both lattices, the E band gap is far narrower than the H band gap and they overlap each other completely. The absolute band gap for the square lattice has a width of $\Delta\omega = 0.027(2\pi c/a)$, and a band gap to midgap ratio of $\Delta\omega/\omega_g = 5.6\%$. For the triangular lattice we have $\Delta\omega = 0.026(2\pi c/a)$ and $\Delta\omega/\omega_g = 6.0\%$.

The dependence of band gap positions on the filling fraction of air cylinders for the E- and H-polarization modes is displayed in Figures 8a and 8b for square and triangular lattices of air cylinders in Tl_3AsSe_3 background, respectively. In both lattice structures, an absolute band gap is present at a filling fraction of $f \geq 0.60$. The optimal absolute band gap lies at $f = 0.72$ for the square lattice with a band gap width of $\Delta\omega = 0.038(2\pi c/a)$ and a band gap to midgap ratio of $\Delta\omega/\omega_g = 7.8\%$. For the triangular lattice the largest absolute band gap lies at $f = 0.79$ with $\Delta\omega = 0.055(2\pi c/a)$ and $\Delta\omega/\omega_g = 11.3\%$.

5 Improvement of absolute band gaps in other complex configurations of anisotropic materials

As noted in Section 3, the quasi–independent adjustment of E and H band gaps can be implemented in 2D uniaxial PBG structures with the extraordinary axis parallel to the cylinders. Although this simplest configuration of anisotropic material is most effective and convenient in improving the absolute band gap, due to the limit of available anisotropic materials and thus for exploiting their

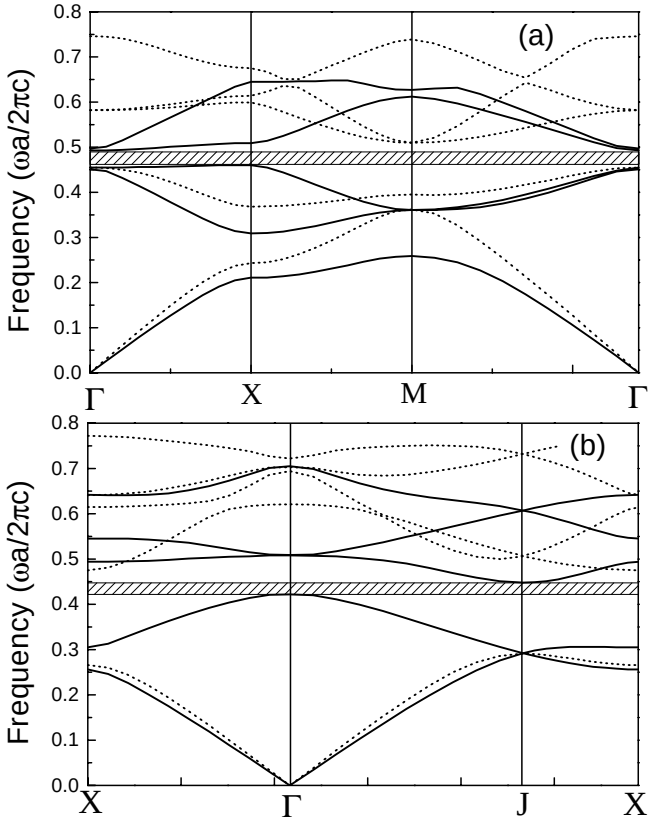

Fig. 7. Calculated photonic band structures of (a) a square lattice; and (b) a triangular lattice of air cylinders in Tl_3AsSe_3 background for E-polarization (solid lines) and H-polarization (dotted lines) modes. The filling fractions of air cylinders in both lattices are $f = 0.7$ and the extraordinary axis of Tl_3AsSe_3 is parallel to the cylinders. An absolute band gap (crosshatched region) is present between $0.466 - 0.493(2\pi c/a)$ in the square lattice and between $0.422 - 0.448(2\pi c/a)$ in the triangular lattice.

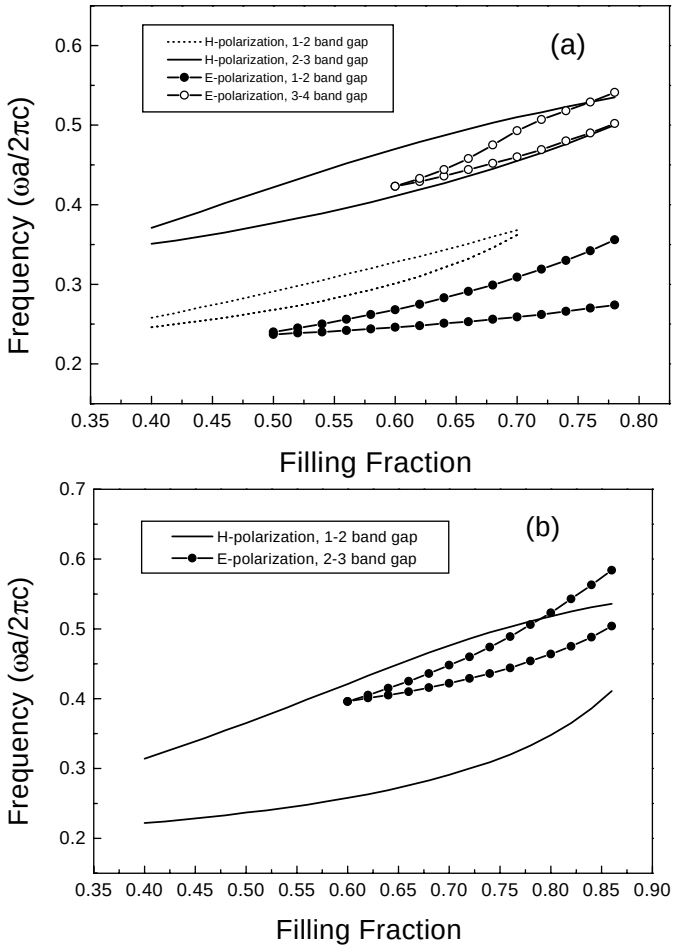

Fig. 8. Dependence of band gap positions on the filling fraction of air cylinders for (a) a square lattice; and (b) a triangular lattice of air cylinders in Tl_3AsSe_3 background. The extraordinary axis of Tl_3AsSe_3 is parallel to the cylinders.

utilization potential as fully as possible, it is reasonable to investigate absolute band gaps in other more complex configurations of anisotropic materials.

Consider, for example, the positive uniaxial crystal Te, which has been shown to be an ideal candidate for 2D PBG structures composed of the lattice of dielectric cylinders in air, due to its large principal refractive index and strong anisotropy. In these structures, the extraordinary axis of Te should be parallel to the cylinders. In contrast, if we choose one of the ordinary axes parallel to the cylinders, then according to equations (4, 5), the refractive index for the E-polarization mode is $n_{\rm o} = 4.8$ while for the H-polarization mode the refractive index is still anisotropic with two principal indices as $n_{\rm o} = 4.8$ and $n_{\rm e} = 6.2$. In a very simplified way, electromagnetic waves at the H-polarization mode will experience an average refractive index (about $(n_{\rm e}+n_{\rm o})/2 = 5.5$) larger than that for the E-polarization mode, then according to the analyses in Section 3, this configuration would be favorable in improving absolute band gaps for 2D PBG structures consisting of lattices of air cylinders in dielectric background.

As noted in Section 2, to demonstrate the existence of a band gap for the H-polarization mode, one can investigate the photonic band structure along the symmetry lines in a fixed region of the Brillouin zone, while permuting the dielectric dyadic elements ϵ_{xx} and ϵ_{yy} in equation (5) [32]. In the following we will apply this method to investigate the anisotropic photonic band structures for the H-polarization mode.

In the square lattice of air cylinders in Te background, we choose an irreducible Brillouin zone where the high symmetry points are coordinated as: $\Gamma = (0,0)$, X $= (\pi/a)(1,0)$, and M $= (\pi/a)(1,1)$. This means that the selected Brillouin zone is prominently along the X-axis. Corresponding to two inequivalent 1/2 Brillouin zones, we have the dielectric dyadic elements in equation (5) as (a) $\epsilon_{xx} = n_{\rm o}^2$, $\epsilon_{yy} = n_{\rm e}^2$; and (b) $\epsilon_{xx} = n_{\rm e}^2$, $\epsilon_{yy} = n_{\rm o}^2$. The photonic band structures in these two inequivalent 1/2 Brillouin zones are displayed in Figures 9a and 9b, respectively for the H-polarization mode. Also plotted are the photonic band structures for the E-polarization mode, which are uniform in the two Brillouin zones. The air cylinders have a filling fraction of $f = 0.7$ and one of the ordinary axes

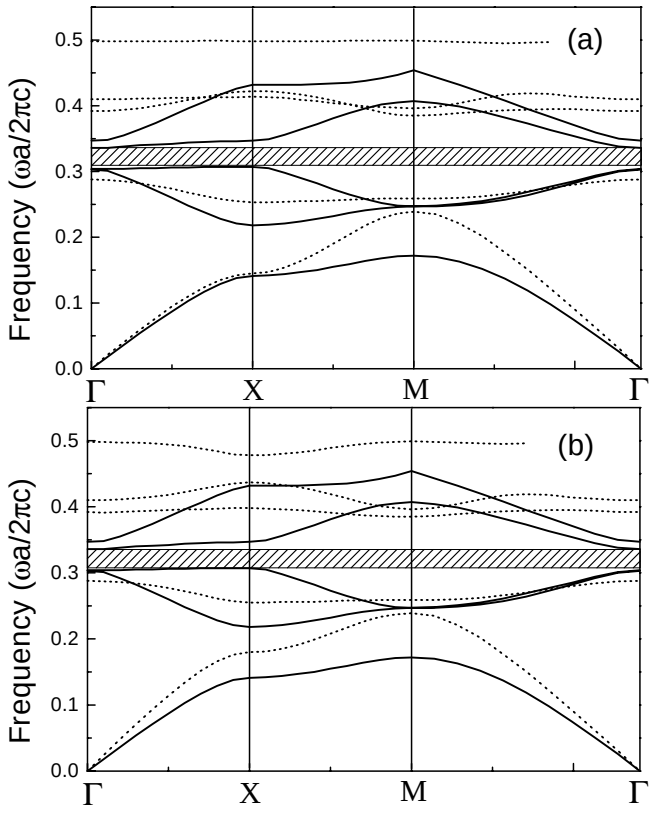

Fig. 9. Calculated photonic band structures of a square lattice of air cylinders in Te background in air for E-polarization (solid lines) and H-polarization (dotted lines) modes in two inequivalent 1/2 partial Brillouin zones of a square lattice as (a) $\epsilon_{xx} = n_{\rm o}^2$, $\epsilon_{yy} = n_{\rm e}^2$; and (b) $\epsilon_{xx} = n_{\rm e}^2$, $\epsilon_{yy} = n_{\rm o}^2$. The high symmetry points of the irreducible Brillouin zone are chosen as $\Gamma = (0,0)$, $X = (\pi/a)(1,0)$, and $M = (\pi/a)(1,1)$. The filling fraction of air cylinders is $f = 0.7$ and one of the ordinary axes of Te is parallel to the cylinders. An absolute band gap (crosshatched region) is present between $0.307 - 0.336(2\pi c/a)$.

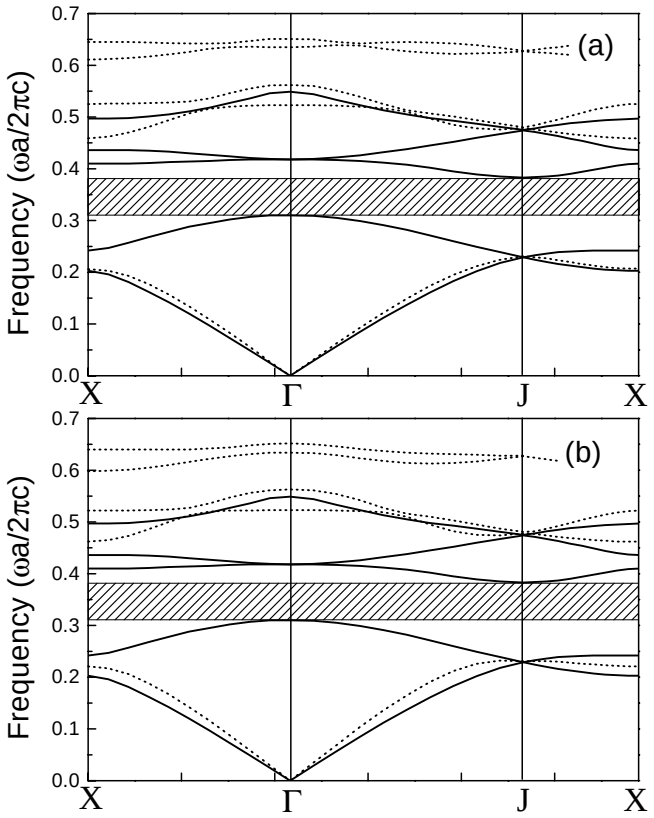

Fig. 10. Calculated photonic band structures of a triangular lattice of air cylinders in Te background in air for E-polarization (solid lines) and H-polarization (dotted lines) modes in two inequivalent 1/2 partial Brillouin zones of a triangular lattice as (a) $\epsilon_{xx} = n_{\rm o}^2$, $\epsilon_{yy} = n_{\rm e}^2$; and (b) $\epsilon_{xx} = n_{\rm e}^2$, $\epsilon_{yy} = n_{\rm o}^2$. The high symmetry points of the irreducible Brillouin zone are chosen as $\Gamma = (0,0)$, $X = (\pi/a)(1,\sqrt{3}/3)$, and $J = (\pi/a)(4/3,0)$. The filling fraction of air cylinders is $f = 0.8$ and one of the ordinary axes of Te is parallel to the cylinders. An absolute band gap (crosshatched region) is present between $0.310 - 0.383(2\pi c/a)$.

of Te is parallel to the cylinders. It is evident from Figures 9a and 9b that in both inequivalent Brillouin zones an absolute band gap is present as the E 3-4 band gap is wholly covered by the wider H 2-3 band gap. Thus an absolute band gap is created in the whole Brillouin zone, which is in fact the E 3-4 band gap. This absolute band gap has a width of $\Delta\omega = 0.029(2\pi c/a)$ and a band gap to midgap ratio of $\Delta\omega/\omega_{\rm g} = 9.0\%$. It should be noted that no band gap is present between the 5th and 6th photonic bands for the E-polarization mode (the 6th photonic band does not include in Figs. 9a and 9b).

Following the similar way, we also select for the triangular lattice of air cylinders in Te background an irreducible Brillouin zone along the X-axis direction, whose high symmetry points have the coordinates as: $\Gamma = (0,0)$, X $= (\pi/a)(1,\sqrt{3}/3)$, and J $= (\pi/a)(4/3,0)$. The photonic band structures in the two inequivalent 1/2 Brillouin zones as (a) $\epsilon_{xx} = n_{\rm o}^2$, $\epsilon_{yy} = n_{\rm e}^2$ and (b) $\epsilon_{xx} = n_{\rm e}^2$, $\epsilon_{yy} = n_{\rm o}^2$ are displayed in Figures 10a and 10b, respectively for the H-polarization mode. As a clarity of view, we plot the photonic band structures uniform in the two Brillouin zones in Figures 10a and 10b, too. The filling fraction of air cylinders is set to be $f = 0.8$. The E 2-3 band gap overlaps completely with a very large H 1-2 band gap, resulting in the presence of an absolute band gap in the whole Brillouin zone. This absolute band gap is essentially the E 2-3 band gap and has a width of $\Delta\omega = 0.073(2\pi c/a)$ and a band gap to midgap ratio of $\Delta\omega/\omega_{\rm g} = 21.1\%$.

In the configuration that one of the ordinary axes of Te is parallel to cylinders, Te can be regarded phenomenally equivalent to a negative material for EM waves. Therefore, the above numerical results are consistent with the general principle for improving the absolute band gap by anisotropic dielectricity in PBG structures, as conceptualized in Figure 4 for lattices of air cylinders in dielectric background. Furthermore, the refractive index and anisotropy in this configuration of Te are both far larger than those of the negative crystal Tl_3AsSe_3, thus it is more favorable for Te to obtain a large absolute band gap than for Tl_3AsSe_3. This enables the full exploitation of

potential utilization of available anisotropic materials in improving the absolute band gap of 2D PBG structures.

The design of absolute band gap in 2D PBG structures fabricated from biaxial crystals can follow quite the similar way. Investigations of absolute photonic band gap in various configurations of biaxial materials can further make full use of anisotropic materials available in nature.

6 Summary and conclusions

In this paper, we have applied the plane–wave expansion method to study the photonic band structures of 2D PBG structures fabricated from anisotropic materials in their various configurations. The numerical simulations show that the anisotropy in material dielectricity for both square and triangular lattices can increase the size of absolute photonic band gap remarkably. As the refractive index for the E-polarization and H-polarization modes can be chosen different, the band gaps can be adjusted and matched to overlap optimally. In particular, the positive uniaxial materials are more favorable in improving the absolute band gap of PBG structures consisting of dielectric cylinders in air, while for crystals composed of air holes in dielectric medium, negative uniaxial materials are more competent. The quasi–independent adjustment of band gaps for the E- and H-polarization modes can be implemented by uniaxial crystals with their extraordinary axis parallel to the cylinders. In order to make a full exploitation of potential utilization for anisotropic materials available in nature we have investigated photonic band structures in other more complex configurations of anisotropic materials, and shown that large absolute band gap can also be obtained in these complex configurations. Due to large varieties of anisotropic materials in nature, this opens up a new scope for designing the band gap of 2D photonic crystals.

This work was supported by National Natural Science Foundation of China.

References

1. J. Opt. Soc. Am. B **10**, 208 (1993), special issue on development and applications of materials exhibiting photonic band gaps.
2. *Photonic Band Gaps and Localization*, Proceedings of the NATO ARW, edited by C.M. Soukoulis (Plenum, New York, 1993).
3. J.D. Joannopoulos, P.R. Villeneuve, S. Fan, Nature **386**, 143 (1997).
4. E. Yablonovitch, Phys. Rev. Lett. **58**, 2059 (1987).
5. S. John, Phys. Rev. Lett. **58**, 2486 (1987).
6. S. John, J. Wang, Phys. Rev. Lett. **64**, 2418 (1990); Phys. Rev. B **43**, 12772 (1991).
7. S. John, T. Quang, Phys. Rev. A **50**, 1764 (1994).
8. J. Wang, Phys. Lett. A **50**, 1764 (1994).
9. S.Y. Zhu, H. Chen, H. Huang, Phys. Rev. Lett. **79**, 205 (1997).
10. E. Yablonovitch, T.J. Gmitter, Phys. Rev. Lett. **63**, 1950 (1989).
11. E. Yablonovitch, T.J. Gmitter, K.M. Leung, Phys. Rev. Lett. **67**, 2295 (1991).
12. E. Özbay, E. Michel, G. Tuttel, R. Biswas, M. Sigalas, K.M. Ho, Appl. Phys. Lett. **64**, 2559 (1994).
13. M. Wada, Y. Doi, K. Inoue, J.W. Haus, Z. Yuan, Appl. Phys. Lett. **70**, 2966 (1997).
14. S.Y. Lin *et al.*, Nature (London) **394**, 251 (1998).
15. T.F. Krauss, R. De La Rue, S. Band, Nature **383**, 699 (1996).
16. U. Grüning, V. Lehmann, S. Ottow, K. Busch, Appl. Phys. Lett. **68**, 747 (1996).
17. K. Inoue, M. Wada, K. Sakoda, M. Hayashi, T. Fukushima, A. Yamanak, Phys. Rev. B **53**, 1010 (1996).
18. H.-B. Lin, R.J. Tonucci, A.J. Campillo, Appl. Phys. Lett. **68**, 2927 (1996).
19. D.L. Bullock, C. Shih, R.S. Margulies, J. Opt. Soc. Am. B **10**, 399 (1993).
20. M. Plihal, A. Shambrook, A.A. Maradudin, P. Sheng, Opt. Commun. **80**, 199 (1991).
21. M. Plihal, A.A. Maradudin, Phys. Rev. B **44**, 8565 (1991).
22. S.L. McCall, P.M. Platzman, R. Dialichaouch, D. Smith, S. Schultz, Phys. Rev. Lett. **67**, 2017 (1991).
23. W.M. Robertson, G. Arjavalingam, R.D. Meade, K.D. Brommer, A.M. Rappe, J.D. Joannopoulos, Phys. Rev. Lett. **68**, 2023 (1992).
24. P.R. Villeneuve, M. Piché, Phys. Rev. B **46**, 4969 (1992).
25. D. Cassagne, C. Jouanin, D. Bertho, Phys. Rev. B **53**, 7134 (1996).
26. R.D. Meade, K.D. Brommer, A.M. Rappe, J.D. Joannopoulos, Appl. Phys. Lett. **61**, 495 (1992).
27. C.M. Anderson, K.P. Giapis, Phys. Rev. Lett. **77**, 2949 (1996); Phys. Rev. B **56**, 7313 (1997).
28. K.M. Ho, C.T. Chan, C.M. Soukoulis, Phys. Rev. Lett. **65**, 3152 (1990).
29. S. Fan, P.R. Villeneuve, R.D. Meade, J.D. Joannopoulos, Appl. Phys. Lett. **65**, 1466 (1994).
30. K.M. Ho, C.T. Chan, C.M. Soukoulis, R. Biswas, M. Sigalas, Solid State Commun. **89**, 413 (1994).
31. Z.Y. Li, J. Wang, B.Y. Gu, J. Phys. Soc. Jpn. **67**, 3288 (1998).
32. Z.Y. Li, J. Wang, B.Y. Gu, Phys. Rev. B **58**, 3721 (1998).
33. Z.Y. Li, B.Y. Gu, G.Z. Yang, Phys. Rev. Lett. **81**, 2574 (1998).
34. *Handbook of Optics*, Vol. II, Devices, Measurements, and Properties, edited by M. Bass (McGraw Hill, New York, 1995), Chap. 33.